Surfaces for heart cells: Establishing the optimum plasma surface engineering methodology on polystyrene for cardiac cell engineering

Maria Kitsara,*[a] Dimitrios Kontziampasis,*[b,c] Efi Bolomiti,[d] Alexandre Simon,[a] Panagiotis Dimitrakis,[d] Antoine Miche,[e] Georgios Kokkoris,[f] Vincent Humblot [e,g] and Onnik Agbulut*[a]

[a.] Sorbonne Université, Institut de Biologie Paris-Seine (IBPS), UMR CNRS 8256, INSERM U1164, Biological Adaptation and Ageing, Paris, 75005, France.

[b.] School of Science and Engineering, University of Dundee, DD1 4HN, Dundee, Scotland, UK.

[c.] Dundee International Institute of Central South University, Tongzipo Road, Central South University, Changsha, Hunan, 410013, P.R. China.

[d.] NCSR Demokritos, Institute of Nanoscience and Nanotechnology, Athens, 15341, Greece.

[e.] Sorbonne Université, Laboratoire de Réactivité de Surface UMR CNRS 7197, Paris, 75005, France.

[f.] School of Chemical Engineering, National Technical University of Athens, 15780 Athens, Greece

[g.] FEMTO-ST Institute, UMR 6174 CNRS, Université Bourgogne Franche-Comté, 15B avenue Montboucons, 23030 Besançon Cedex, France.

*Corresponding Authors:

Dr. Maria Kitsara, kitsara.m@gmail.com

Dr. Dimitrios Kontziampasis, dkontziampasis001@dundee.ac.uk

Prof. Onnik Agbulut, onnik.agbulut@sorbonne-universite.fr

Abstract

Plasma surface modification is a popular method for improving cell culture on surfaces, and polystyrene (PS) is literature's material of choice. This study identifies the optimum plasma treatment for promoting normal cardiac cell behaviour during culture. PS slides were plasma-treated with O_2, N_2, O_2+N_2 and Ar+N_2 for 20 and 30 min in a reactive ion etcher (RIE). SEM reveals that O_2 and O_2+N_2 plasma create dual scale roughness, N_2 plasma creates oval-shaped structures, while Ar+N_2 exhibits no topography. Evaluation by XPS reveals an increase in the atomic percentage of oxygen for all treatments. Contact angle measurements agree as all treatments lead to hydrophilisation, with N_2 samples exhibiting long-term stability.

Two sources of cells were used to identify the optimum plasma treatment for cardiac cell culture on PS. H9c2 cells exhibit optimal behaviour with N_2 and N_2+Ar regarding viability, morphology, and focal adhesion contact. The same was observed for primary cardiomyocytes on N_2 samples. For purified cardiomyocytes, immunofluorescence revealed well-organised sarcomeric structure on N_2 samples, exhibiting clear improvement compared to control. SEM validated these findings, as cardiomyocytes on N_2-treated PS exhibited physiological, elongated shape. These findings provide solid evidence that the optimum treatment for PS is the use of N_2 plasma.

1. Introduction

Polystyrene (PS) is currently one of the most widely used polymers, mainly due to its advanced mechanical properties and low cost of production [1–3]. PS can be naturally transparent and non-toxic to cells, and for these properties it has prevailed as a biomaterial that is used in biomedical research [4,5]. Even though the use of PS in standard clinical practices is not widespread, it poses as the material of choice for petri dishes, test tubes, and well plates for cell, tissue, and bacterial growth [6]. As a polymeric material however, PS has an intrinsic hydrophobicity and low surface energy, while simultaneously lacks the desired surface chemistry that favours cell attachment, spreading, and proliferation.

In order to maintain all the desired properties for the material and solve the previously mentioned problems in cell affinity and final compatibility, the route of surface modification is typically followed. In recent studies, chemical (for example grafting, oxidation, sulfonation, crosslinking, etching) and physical (for example electron or ion beam, laser treatment, sputtering) techniques are utilised for the surface modification of polymers [7–20]. Comparing to all the aforementioned approaches, plasma surface modification shows a unique dual capability of homogeneous and simultaneous modification of both surface chemistry and topography [21,22]. Plasma, in numerous studies, has been used as a tool to alter and enhance the surface properties of a plethora of polymers in order to promote their use for biological and biomedical applications, either via removing or by depositing material on the surface [23–26]. In order to provide the material under treatment with the necessary chemical cues and allow it to promote specific cell functionalities, two routes are the most widely used in plasmas. The first and most used one is O_2 plasma treatment (or etching), which increases the –OH, =O and other oxygen groups, while additionally it creates structures on the polymer surface as proven in the literature [23,27–29]. N_2 plasma poses as the second most used route, and its use increases the $–NH_2$, =NH, ≡N, and amines on the surface. The latter treatment appears less invasive in terms of modifying the topography of the material [30,31]. Especially for PS, various studies have provided insights on how different plasmas invoke different changes on its surface properties, i.e. surface chemistry and topography [6],[32–40]. Recent initial studies, have started to investigate the effect of plasma surface modification on PS for controlling cultured cell functions [11,41].

Haubenwallner et al. suggested that there is a direct connection of cell fate to the polymer niche [42]. In their study, they reveal that the use of a specific type of polymer with a tailored microenvironment can be considered as an effective tool for promoting essential cell characteristics for subsequent approaches and point out the necessity of using a cell type specific screening approach when referring to synthetic materials and material treatments for particular cell types. This indicates that previously described treatments for a specific type of cell will unlikely be appropriate for another type,

or for triggering a similar behaviour of the cell, showcasing that there is no global solution. They point out that every type of cell and tissue prefers a different microenvironment.

Cardiac cell engineering has also signalled the need of identifying and decoding an optimum plasma surface modification in order to obtain a microenvironment that shows improved attachment, morphology, and protein expression. This is essential for understanding and investigating the pathologies of the heart in culturing plates (disease modelling), as well as the effect of drugs on normal behaving cells and tissues, and it is a vital step towards the 'heart on a chip' integration [43,44].

The current study aims to address this knowledge gap, and tailor an optimum surface for cardiac cell engineering, via modification of PS. This will be achieved by bringing together the two most widely used components in terms of material (PS) and surface modification method (plasma). The aspiration is not only to characterise the topographical or chemical changes induced by the plasma treatments on the surface of PS, but to additionally investigate the cardiac cells' response to these changes. This will allow for an understanding of which route favours the normal function of the cardiac cells. The focus of the current study is on cardiac cell culture, and the ultimate goal is to provide an integrated systematic study from both the materials and biological perspective, when using the three most common plasma treatments to modify the favourite material in biological research. These treatments are namely O_2, N_2, and Ar plasma.

Since PS poses as the main material for cell culture dishes and plates, its cytocompatibility is very well known. Even though it can be used as is for several types of cells, this is not the case for cardiac cells. Cardiac cells are very selective and require a pre-treatment with coating before culture, which is based on extracellular matrix proteins. In addition, to the best of our knowledge, there is no report in literature that has studied the effect of plasma treatment of PS on primary cardiac cell function. Herein, we culture two different types of cells on numerous plasma-treated PS surfaces without any pre-treatment with extracellular matrix proteins. Initially, the cell line H9c2 was studied, which is derived from an embryonic rat heart. This was necessary for acquiring useful information on the viability and cell stress using a big batch of cells, which are easier to culture. Subsequently, we moved forward to the culture of primary cardiomyocytes that were derived from neonatal rat hearts, culturing both non-purified and purified cardiomyocytes. The former culture was a mixture and contained other types of cardiac cells, i.e. fibroblasts, endothelial cells, and smooth muscle cells.

2. Materials and methods

2.1. Materials

PS slides were purchased from Thermo Fisher Scientific®, (nunc, 960004), which were pre-treated for cell culture by the manufacturer.

2.2. Plasma treatment

PS slides were plasma-treated using O_2, N_2, O_2+N_2 and Ar+N_2 gas mixtures in a reactive ion etching (RIE) tool (Alcatel Nextral NE330). This reactor is producing by the application of a radio frequency (RF) power, a capacitively coupled plasma discharge. The chamber of the plasma reactor (see Fig. S1†, ESI), which is 420mm in diameter, was cleaned by O_2 plasma before the PS samples were introduced for treatment to avoid any contamination from previous treatments. Taking into account the chamber size, a set of 10 slides with the same interspace distance were treated in each experiment. The RF biased electrode, on top of which the slides are put, carries a quartz cover plate (see Fig. S1†, ESI).

The feed gas mixture and the operating conditions were chosen in accordance with treatments reported in literature [21,22]. O_2, N_2, and mixtures of O_2 with N_2 and Ar with N_2 were utilised. The feed of the reactor was 100 sccm for O_2, 50 sccm for N_2, and 100+50 sccm for O_2+N_2 and Ar+N_2, respectively. The pressure in the reactor was kept at 20 mTorr and the generator power was 200 W. The treatment time was 20 and 30 min, and the reasons for choosing the are the following. In the

case of oxygen plasma, we are awar that in order to achieve the dual scale structures, which will have the desired effects in this specific reactor (Nextral 330, RIE from Alcatel), we needed to etch for long times, in the region of tens of minutes, so 20 and 30 minutes fell into that window of values [45–47].

Additionally, we have chosen to use 20 and 30 minutes of treatment in order to achieve surfaces with stable surface chemistry over time. Indeed, we have found that the 30 min of nitrogen plasma treatment led to the creation of stably hydrophilic surfaces. This is important for the current research, as having samples that are stable over the time of the study is necessary, especially since there are repeated cell culture studies that need to be performed at different time periods and at different intervals from the plasma treatment of the samples.

In parallel, for the case of nitrogen plasma, these times allow for “big enough” nanostructures to be created with plasma. It was found in initial experiments that for approximately 10-15 minutes the corresponding nanostructures created on the surface were not sufficient to invoke the desired effect on wettability, as it was with the case of oxygen. Combining all of the above, it was chosen to use 20 and 30 minutes etching times for all the plasma treatments in this study.

It should be stressed that every 3 min the plasma process was stopped for 2 min in order to prevent the heating of the quartz substrate of the plasma reactor. Heating of the quartz substrate originates from the power deposited by the plasma generated charged species (ions and electrons). The power density deposited depends on the ion and electron energies and flux and is measured or estimated from hundreds of mW/cm2 to 1 W/cm^2 [48,49]. After plasma treatment, the samples were kept in a sealed box in a room with controlled temperature and humidity (20^{o}C, relative humidity (RH) 40%).

2.3. Scanning electron microscopy (SEM)

SEM was used to visualise the structures of the plasma-treated PS (Gemini SEM 500, Zeiss). The samples were sputtered with a thin platinum layer prior to SEM observation using the ACE600, Leica. Images at different magnifications were obtained on at least five different areas of the same sample and in three different samples with the same conditions for statistical analysis. The images were acquired by applying beam voltage of 3 kV and using InLens detector.

2.4. Wettability assessment

Water contact angle (WCA) measurements were performed using the DSA 30 system from Krüss. The sessile drop method was used, and the measurements took place at room temperature (20 ^{o}C). The volume of the applied drops of deionised water was 1 μl, and the WCAs were measured 10 seconds after drop deposition. WCA data were obtained by averaging over several measurements in different areas on the sample’s surface.

2.5. X-ray Photoelectron Spectroscopy (XPS)

XPS analyses were performed using an Omicron Argus X-ray photoelectron spectrometer, equipped with a monochromated AlKα radiation source (hv = 1486.6 eV), and a 280 W electron beam power. The emission of photoelectrons from the sample was analysed at a takeoff angle of 45° under ultra-high vacuum conditions (≤10−9 mBar). Spectra were carried out with a 100 eV pass energy for the survey scan and 20 eV pass energy for the C 1s, O 1s, and N 1s regions. Binding energies were calibrated against the C 1s (C-C) binding energy at 284.8 eV and element peak intensities were corrected by Scofield factors. The peak areas were determined after subtraction of a shirley background. The spectra were fitted using Casa XPS v.2.3.15 software (Casa Software Ltd, U.K.) and applying a gaussian/lorentzian ratio equal to 70/30.

2.6. H9c2 cell culture

The H9c2 cell line, derived from embryonic rat heart tissue, was cultured in high glucose DMEM + Glutamax supplemented with 10% foetal bovine serum and 1% penicillin/streptomycin. Cells (1 x

10^5) were seeded on the PS samples after passage using trypsin-EDTA. After two days of culture, scaffolds were washed with PBS and the cells were fixed with 4% paraformaldehyde solution.

2.7. Isolation of neonatal rat cardiomyocytes

Newborn rat cardiomyocytes (NRCMs) were obtained from 1-day-old Wistar RjHan rat (Janvier Labs, Saint-Berthevin, France). The hearts were cut in small pieces and the cardiac cells were isolated, using a neonatal heart dissociation kit (Miltenyi Biotec, Paris, France) following the manufacturer's instructions. Cardiomyocytes were purified by depletion of non-target cells (such as fibroblasts, endothelial cells), using a neonatal cardiomyocyte isolation kit (Miltenyi Biotec, Paris, France). 5 x 10^5 cells were seeded on $2cm^2$-PS pieces and cultured with DMEM medium (with 4.5g/L D-Glucose and without Na Pyruvate) supplemented with L-glutamine, penicillin-streptomycin, 10% horse serum and 5% fetal bovine serum (FBS) at 37 °C and 5% CO_2 for 3 days. All animal studies were approved by our institutional Ethics Committee "Charles Darwin" and conducted according to the French and European laws, directives, and regulations on animal care (European Commission Directive 2010/ 63/EU) under the license B75.13.20.

2.8. Viability and oxidative stress assay

The viability of both H9c2 and NRCMs was assessed by using the Muse® Count & Viability Kit. The kit differentially stains viable and non-viable cells based on their permeability to the two DNA binding dyes present in the reagent. The oxidative stress of the H9c2 cells was calculated by using the Muse® Oxidative Stress Kit, which allows for the quantitative measurements of Reactive Oxygen Species (ROS), namely superoxide radicals in cells undergoing oxidative stress. The assay provides the relative percentage of cells that are ROS negative and positive. The measurements were repeated 3 times, using 2 samples per case.

2.9. Immunostaining and cell morphology analysis

All cells were washed with PBS and fixed with 4% paraformaldehyde solution. After 3 washing steps, they were incubated with 5% bovine serum albumin (BSA) for 1 hour. H9c2 cells were incubated for 90 minutes at room temperature with an antibody against vinculin (mouse IgG1, dilution 1:200, Sigma-Aldrich, Saint-Quentin-Fallavier, France). After 3 washes in PBS, the H9c2 cells were incubated in the secondary antibody (Alexa 488 goat-anti-mouse, dilution 1:1000, Life Technologies) and Alexa Fluor® 647 Phalloidin (Life technologies). NRCMs were incubated for 90 minutes at room temperature with antibodies against α-actinin (mouse IgG, dilution 1:300, Sigma-Aldrich, Saint-Quentin-Fallavier, France) and fibronectin (rabbit IgG antibody, dilution 1:50, Santa Cruz Biotechnology, Heidelberg, Germany). After 3 washes in PBS, NRCMs were incubated in the presence of secondary antibodies (Alexa 488 goat-anti-mouse and Alexa 568 goat-anti-rabbit, dilution 1:1000; Life Technologies). All the samples were mounted with mowiol containing 5 µg/ml Hoescht 33342 (Life Technologies). Images were captured using a motorised confocal laser scanning microscope (Leica TCS SP5).

2.10. Statistical analyses

Groups were statistically compared with GraphPad Prism 7 using ordinary one-way analysis of variance. The normality was checked using the Shapiro-Wilk normality test. If the normality of distribution assumption was not met, the nonparametric Kruskal-Wallis test was used instead of an ordinary ANOVA test. If a significant difference was found, then multiple comparison tests were performed to compare the different groups analysed (Dunn's or Tukey multiple comparison test following a nonparametric or parametric test, respectively). A p-value ≤ 0.05 was considered significant. Values are given as the means ± standard error of the mean (SEM).

3. Results and discussion

3.1. Assessment of roughness and hydrophilicity changes to PS by plasma treatment

As it is mentioned in the introduction, plasma treatment of polymers leads to the formation of structures on their surface. The reasons behind this formation of structures, have been analysed in literature extensively [50–54]. In this work, we validate differences on these structures via using SEM to examine samples that have undergone different plasma treatments. Since the focus of this work is to identify the optimum plasma treatment for cardiac cell culture, one can clearly distinguish different morphologies of topography on the surface of PS for the different plasma treatments, comparing the average size of structures as they appear in the acquired SEM images.

Electron microscopy of the samples (Fig. 1) shows that in the case of O_2 plasma treatment, there is dual scale roughness created. Islands of flower-like structures, having a size in the region of several hundred nm to a few μm size, can be identified. Additionally, one can clearly notice the presence of round and oval-shaped nanostructures with 20-30 nm diameters, scattered uniformly across the surface. The aforementioned flower-like morphology is similar (although not identical in shape) to the one reported for O_2 plasma treatment of PMMA (poly-(methyl methacrylate)) when using the same reactor [22]. In the case of O_2 plasma treatment, the size of the large nanostructures increases from average maximum dimensions of ~115 nm width and ~120 nm length to 170 nm width and 200 nm width when plasma treatment time increases from 20 to 30 min. The underlying small nanostructures that appear in the background are not affected from the increase in treatment time. When a mixture of N_2 and O_2 is used for the plasma treatment of PS, microscopy indicates the same type of dual scale roughness on its surface, *i.e.* the formation of flower-like islands and small underlying nanostructures. The size of the islands increases to ~160 nm width and ~180 nm length to 270 nm width and 280 nm width for the 20 min and 30 min plasma treatment samples, respectively. Taking into consideration the trend of increasing dimensions of the structures on the PS surface when increasing time, and adding the fact that O_2 plasma treatment leads to the formation of an identically shaped morphology, one can hypothesise that the nitrogen ions act in a catalytic fashion on the reactive oxygen ion etching in the case of PS.

In the case of N_2 plasma treatment, SEM shows a different type of structures on the PS surface (Fig. S2† contains images at higher magnifications for better visualisation). There, we can identify closely packed round and oval-shaped nanostructures present over the whole polymer surface, which have a diameter of ~35 nm and ~45 nm for 20 min and 30 min treatment times respectively. When N_2 and Ar mixture is used for the treatment of PS, SEM images show that there is a minor change in the topography of the surface. Even at high magnifications, (Fig. S3†), there is no measurable change on the surface. Only the nanosized structures due to sputtering before SEM imaging appear, similarly with the untreated PS SEM image (Fig. S4†). SEM of untreated PS showed a flat surface (with some stochastic nanostructures due to sputtering before SEM), showcasing that the structuring of the PS surface resulted from the effect of plasma etching.

If one were aiming to illuminate the mechanisms behind the formation of the different surface morphology, a multiscale modeling framework linking with predictive capabilities would have been required. This framework should link the operating parameters of the plasma reactor or the plasma parameters with the surface morphology [53]; critical for this framework is the accuracy and the validity of the model used for the description of the surface morphology (e.g., cell based description of a Monte Carlo model). However, this would have diverted this research away from its aim, and is not considered further in the current study, and will be followed up in a future publication.

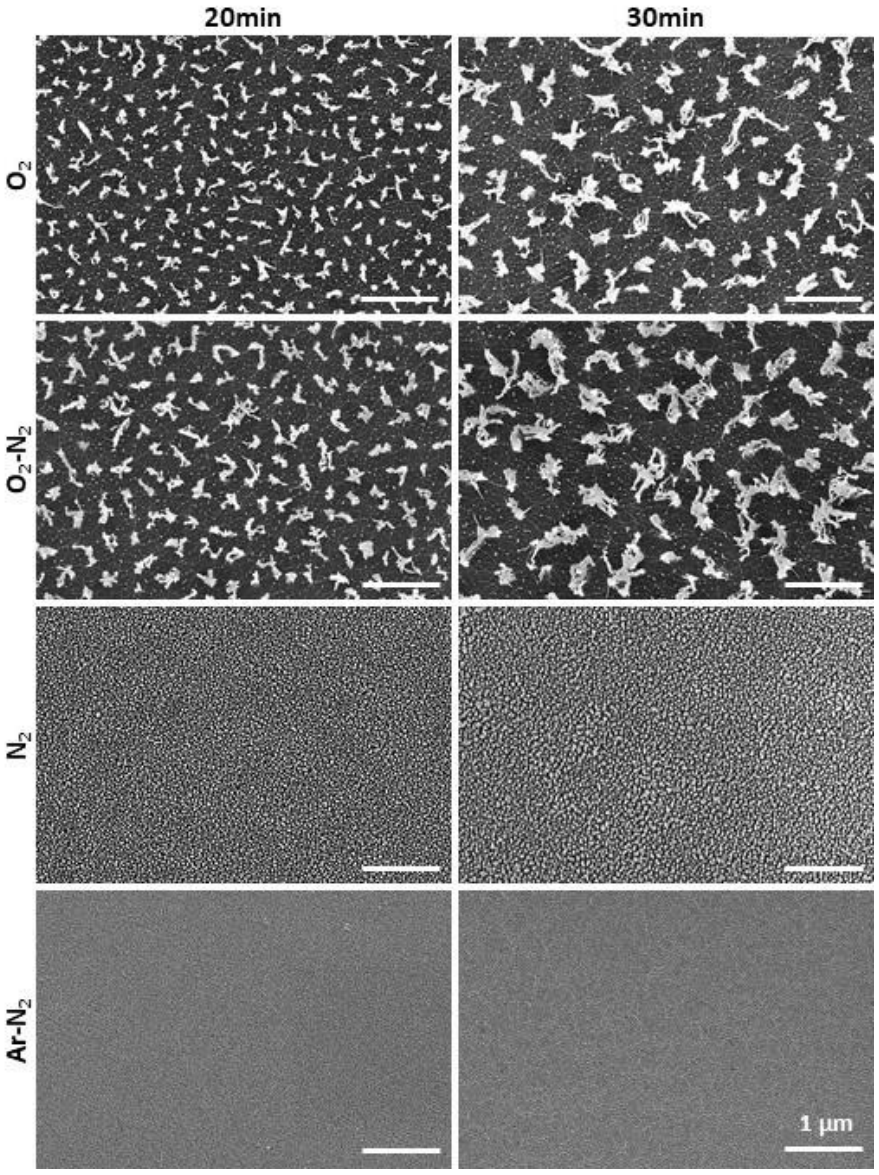

Fig. 1. Morphology of plasma-treated PS slides. SEM images of PS slides, undergone various plasma treatments after 20 min (left column), and 30 min of exposure (right column).

The wettability of the plasma-treated PS was evaluated by WCA measurements (Fig. 2). The WCA of the commercial PS slides was found to be ~ 70°, a value that is lower than that of pure PS (~90°) [55], but still not hydrophilic. Following plasma treatment, all the samples rendered to superhydrophilic immediately, with the exception of the Ar-N_2 treated sample. Subsequently, the ageing of the plasma-induced surface wettability was examined for a period of more than one month of storage under controlled conditions (20°C, RH 40%). It was observed that most of the samples started gradually to become less hydrophilic over time. Only the N_2-treated samples were an exception and remained stably superhydrophilic for a period of more than one month. It is very interesting to note that the 20min O_2-treated samples exhibited a highly progressive recovery of the WCA. The WCA measurements also showcased that in all samples – except for the N_2 ones - there is a clear difference between the 20 and 30 mins of treatment with plasma. The longest plasma treatment assisted to a longer-term hydrophilicity, which in the case of N_2 led to a "stably-hydrophilic" surface (see also Fig. S5† and movie M1).

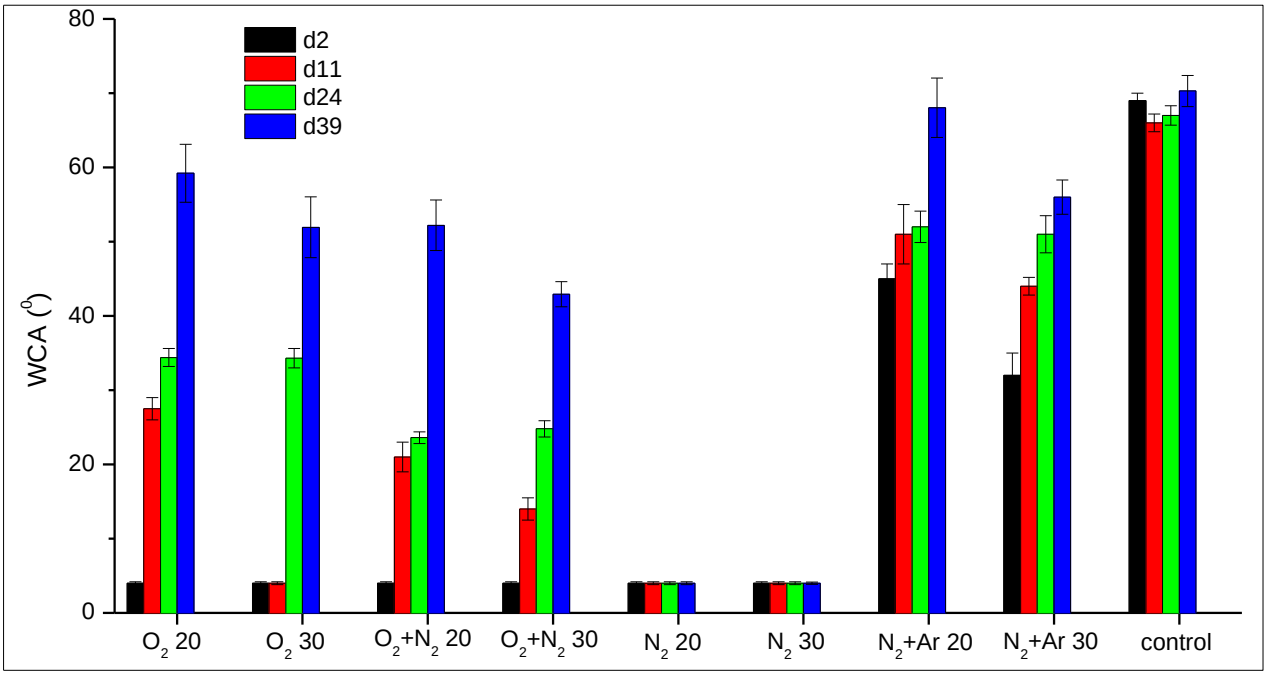

Fig. 2. Hydrophilicity of plasma-treated PS slides. Mean apparent ~~water contact angle~~ WCA of plasma-treated PS slides at different periods. dx stands for the measurement at day x after plasma treatment.

3.2. Evaluation of PS surface chemistry after modification with various plasma gases

XPS measurements were also performed in order to assess the validity of plasma treatments. Figure S6† presents the survey spectra of the untreated PS sample (control) versus the treated ones with different plasma conditions. On the control spectrum, one can clearly see the strong C1s contribution at 285.0 eV, together with a non-negligible O1s contribution at 530.0 eV, representing almost 14 % in elementary composition (Table 1). The presence of oxygen in the control strongly suggests that the slides surface does not contain only pure PS. This is expected as according to the manufacturer the slides were treated for cell culture. However, further information on the type of treatment is not provided. Also, the fact that the samples were not kept under vacuum increased a possible contamination from air.

After 30 minutes of pure O_2 plasma treatment, the atomic percentage of the O1s contribution rises to 38.3 % (Table 1), which is within the values reported for similar treatments and the equivalent time of plasma processing [56,57]. Regarding N_2 plasma treatments, several combinations were tested, pure N_2, O_2+N_2 and Ar+N_2. All three conditions show the presence of N1s on the survey spectra (Fig. 6†) within different proportions. When nitrogen is mixed with oxygen for the plasma, due to oxygen being more reactive than nitrogen, only a small quantity of nitrogen is found on the surface after activation (1.1 %) and the resulting spectrum is very similar to the one obtained for standalone O_2 plasma treatment. However, the use of either pure N_2 or the one mixed with Ar, leads to up to 10.0 % of N_2 present on the PS surface in the best-case scenario (Fig. 6† and Table 1). It should be noted that also in the case of using Ar, the measured amount of oxygen is higher than the non-treated sample.

For the cell culture experiments, it was decided to concentrate only on the pure plasma treatments, either O_2 or N_2. Therefore, the high-resolution XPS spectra obtained for C1s, N1s and O1s for these conditions are presented on Figure 3. The high-resolution XPS spectra of Ar-N_2 are quite similar to the N_2 ones and have added at the EIS (Fig. S7†). As mentioned previously, the C1S region for the control sample exhibits few contributions from pure PS (284.8 eV for aromatic carbon atoms and C_C, C_H bonds of the lateral chains of the polymer and 291.5 eV corresponding to the aromatic shake-up contributions representing around 5-10 % of the total C1s intensity) [58], but also some contributions due to the treatment by the manufacturer and the storage conditions [57].

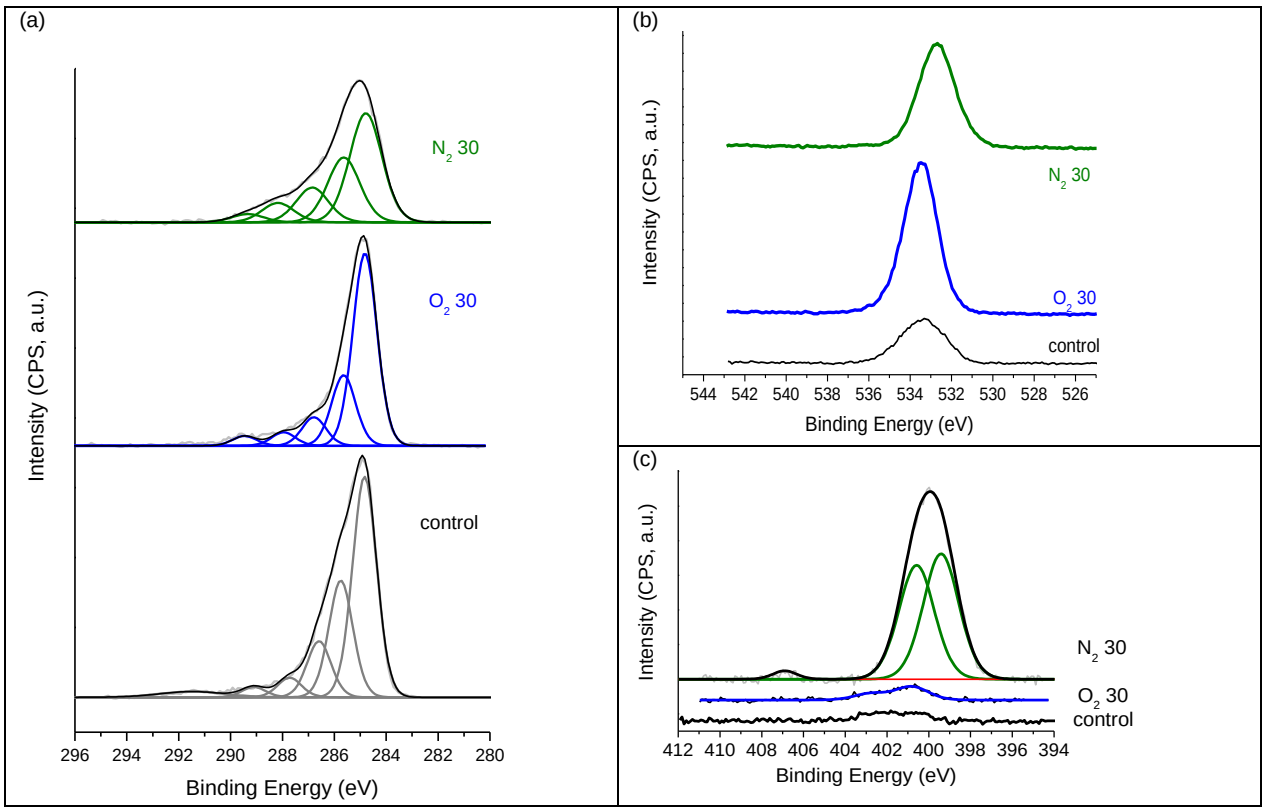

Fig. 3. Evaluation of plasma-treated PS surface chemistry. High Resolution XPS spectra of untreated PS (control) and treated with O_2 and N_2 plasma for 30 minutes (O_2 30 and N_2 30, respectively): (a) C1s, (b) O1s and N1s.

After (O_2 or N_2) plasma treatments, the associated spectra exhibit differences both in shape but also in chemical composition. Following O_2 plasma, the spectrum is dominated by 2 strong contributions at low binding energy, assigned to the C-C, C-H and aromatic carbon atoms (284.9 eV, 61.1 at. %), and to carbon atoms linked oxygen species (285.7 eV, 22.4 at. %). These results are in good agreement with previous studies [58]. We noted that the related O1s spectrum (Figure 3b), exhibits a thin sharp peak centred at 533.0 eV, suggesting oxygen species of the same chemical nature.

For N_2 treatment, the C1s spectrum exhibits a more enlarged peak with several contributions arising from either N species or O species for binding energies contributions encompassed between 285.0 and 288.0 eV (Table 2) [57,58]. This spectrum is much more complicated to analyse due to the presence of multiple possible species, confirmed by a wide O1s peak (Figure 3b). In fact, the different contributions are linked to the chemical environment of a given atom and the associated chemical bound. Therefore, the more different chemical environments are present, the larger the peak will appear. As a result, starting with a complex surface chemistry as observed for the PS control, after plasma reaction, multiple new species will be formed upon this chemical reaction. This will have a consequence of enlarging peaks' contributions (the full width at half maximum increases) and also of energy shifts of the contributions due to difference in electronegativity of the atomic environments. This is also visible on the N1s spectrum (Figure 3c) with a large peak in the 401.0 eV region, composed of two equivalent contributions for charge and neutral nitrogen species [57], but also with the presence of a small contribution at higher binding energy (408.0 eV) usually assigned to NO_x species [59].

Summarising, the XPS results that are obtained for the different untreated and treated PS surfaces, appear in agreement with the wettability measurements that are presented above, and can confirm the initial hypothesis that activation by plasma treatment is a promising treatment method for the creation of PS biocompatible surfaces.

Table 1 Summary of PS atomic composition derived from XPS analyses.

Plasma treatment	Atomic composition %		
	N 1s	**O 1s**	**C 1s**
Ar+N_2 20 min	6.4	22.9	70.7
Ar+N_2 30 min	9.7	40.3	50.0
N_2 20 min	9.9	31.3	58.8
N_2 30 min	10.1	28.5	61.4
O_2+N_2 20 min	1.1	26.4	72.5
O_2+N_2 30 min	1.1	41.3	57.6
O_2 20 min	0	23.6	76.4
O_2 30 min	0	38.3	61.7
control	0	13.9	86.1

Table 2 Summary of binding energies (BEs) and functional groups from the high resolution XPS scan results (C1s, N1s, O1s) of the PS before and after O_2 and N_2 plasma treatments. For the O1s region, the eV values are given for the apex of the spectrum. (Table S2† presents both element by element 100 % and the whole elements.)

Samples	**Assign.**	C-C, C-H	C-O, C-N, C-O-C	C=O, N=C	O=C-O, O=C-N	CO_3^-	π-π*	N-CO	$^+$N-C	NO_x	*C=O, C-O, CO_3^-
control	**BE (eV)**	284.8	285.7	286.6	287.7	289.1	291.5				533.3
	Atomic %	43.0	22.7	11.0	3.8	2.0	3.0	0.6			14.0
O_2 30 min	**BE (eV)**	284.8	285.6	286.8	288.0	289.5					533.5
	Atomic %	37.4	13.7	5.6	2.6	1.9		0.8 0			38.0
N_2 30 min	**BE (eV)**	284.8	285.6	286.9	288.2	289.4		400.8	402.0	408.4	532.7
	Atomic %	28.6	17.0	9.1	5.1	2.2		5.2	4.7	0.2	27.8

3.3. Influence of plasma gas on H9c2 cells viability and oxidative stress

Even though PS cytocompatibility is well known, to the best of our knowledge, there is no report scrutinising the effect of plasma treatment of PS on cardiac cells function. In order to evaluate the impact of plasma treatment of PS on cardiomyocyte viability and morphology, we firstly utilised the H9c2 cell line, which is isolated from the embryonic rat heart tissue. This well-characterised cell line was used for acquiring useful information on the viability and cell stress, via using a big batch of cells [60]. H9c2 cells viability was determined after 2 days in culture on different plasma treated PS samples. Quantification of live cells using the Muse® Count & Viability Kit showed that the number of viable cells was lower for O_2-treated surfaces, compared to N_2 or Ar+N_2 treated surfaces although the difference did not reach statistical significance (Fig. 4). In parallel to this measurement, the oxidative stress of the H9c2 cells was calculated by using the Muse® Oxidative Stress Kit, which allows for the quantitative measurements of ROS. As demonstrated in Figure S8†, the relative percentage of ROS positive cells were increased in O_2-treated surfaces.

The morphology of H9c2 that were cultured on plasma-treated PS was evaluated using immunofluorescence imaging. Figure 5 shows confocal microscopic images after immunostaining for vinculin and staining for F-actin, and nuclei of H9c2 cells on the PS samples (see supplementary movies in the ESI). Evidently, the cells were spread all over the samples and show a nice structure of their actin filaments in the control, as well as the N_2 and Ar+N_2 treated samples, but not in the O_2

treated samples. The vinculin immunostaining indicates the focal adhesion contacts of the cells to the substrate. Vinculin is a cytoplasmic actin-binding protein enriched at both cell-cell and cell-matrix adhesions [61,62]. It is evident in the images that cells adherent to the N_2-treated samples displayed prominent vinculin staining in focal contacts, which is more intense in the 30-min treated ones. In contrast, the cells that were cultured on the O_2-treated substrates displayed much less organisation of vinculin to focal contacts and an increased diffuse cytoplasmic vinculin staining, accompanied by short and disrupted actin bundles. The rest of the surfaces exhibit vinculin focal contacts, but do not appear as strong as the N_2-treated ones. These results are in agreement with a previous study that reported the effect of nanotopography on H9c2 cell viability in the case of tantalum-based nanodot arrays [63]. There, they observed that vinculin immunostaining was widely distributed within cells grown on flat surfaces and up to 50-nm nanodot arrays, whereas it was dramatically decreased for the 200-nm nanodot samples. In the current study, the N_2-treated surfaces have nanostructures that are at the range of 45 nm, while the O_2 and O_2+N_2 have quite larger ones (more than 100 nm).

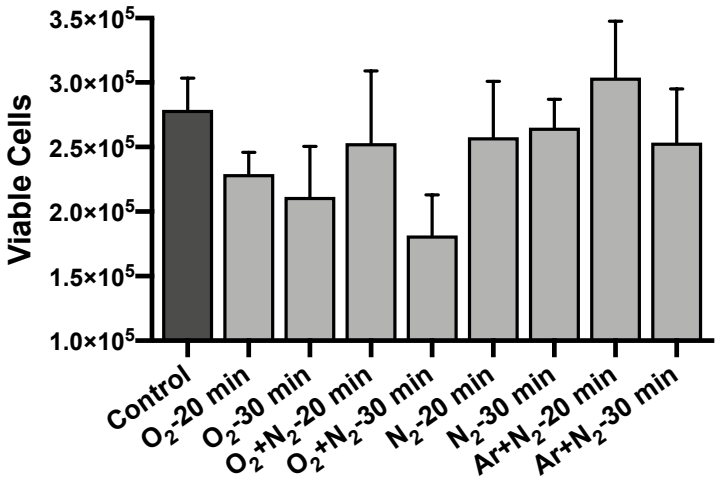

Fig. 4. Cell viability monitoring of H9c2 cells cultured on different plasma treated PS. Two days after cells seeding on various plasma-treated PS, live cells were quantified using the Muse® Count & Viability Kit. Statistical analyses were realised using non-parametric Kruskal–Wallis test.

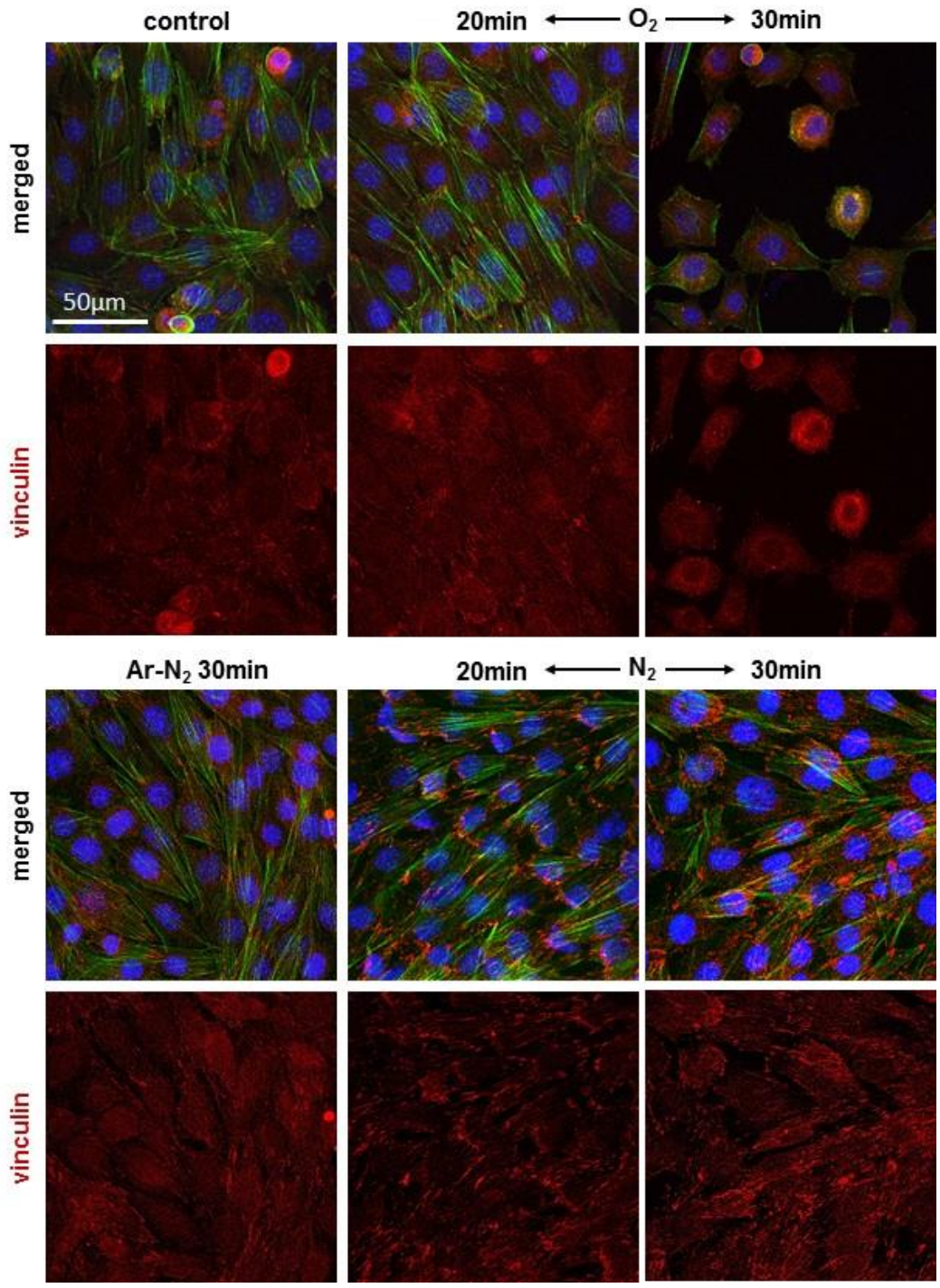

Fig. 5. H9c2 cells morphology on plasma-treated PS. Fluorescent images of H9c2 cells cultured on control and plasma-treated PS for 2 days. Green: F-actin, red: vinculin, blue: nuclei.

3.4. N_2 plasma treatment favours cardiomyocytes viability and morphology

To confirm that the optimum plasma treatment of PS for cardiomyocyte culture is with N_2 gas, primary cardiomyocytes from neonatal rat hearts were cultured for three days on the plasma-treated PS surfaces. In these experiments, we used both non-purified and purified cardiomyocytes, and their viability was determined after 3 days in culture.

Initially, we characterised the PS surfaces without plasma treatment in order to assess the cardiomyocytes' viability and function. Quantification of live cells using the Muse® Count & Viability Kit showed that the number of live cells was lower in the case of the purified cardiomyocytes (Fig. 6a). These results are expected due to the proliferation capability of some cells that are present in this case, and mainly of fibroblasts. It must be noted that cardiomyocytes do not proliferate and their

culture is characterised as quite selective in comparison to other types of cells, due to their difficulty to adhere and spread *in vitro*. For this experiment, we performed double immunostaining of α-actinin and F-actin in order to distinguish the cardiomyocytes in the non-purified cells (Fig. 6b,c). Actin fibers are present in all types of cells, while α-actinin exists exclusively in the cardiomyocytes. These images show clearly that the presence of the other cell populations aids significantly in the survival of the cardiomyocytes, which happens even in the case of the O_2-treated samples. The sarcomeres have better structure as it is revealed by the immunostaining with α-actinin in the Fig. 6b that in the Fig. 6c. The microscopy analysis is in total agreement with the viability results as can be seen in the figures.

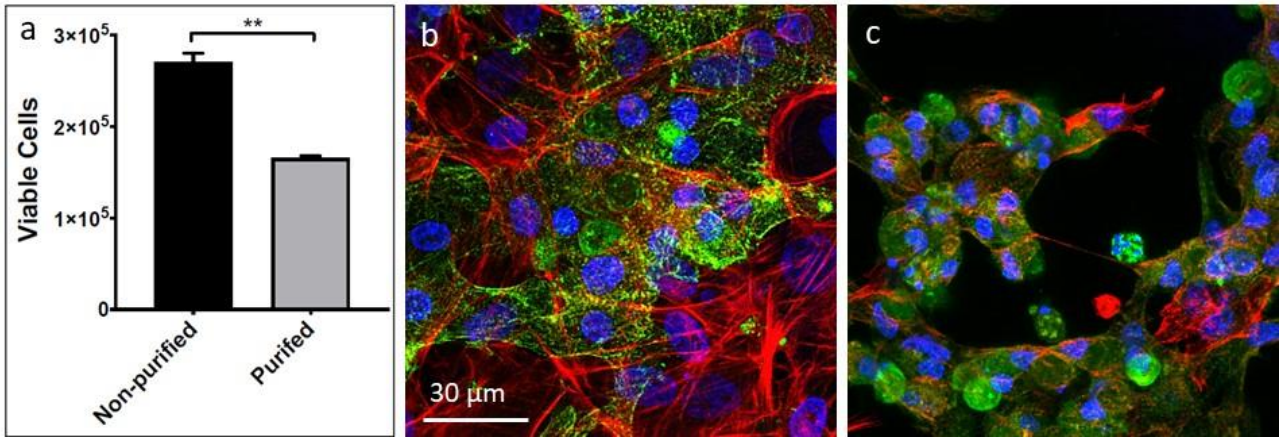

Fig. 6. Cell viability and morphology assessment of primary cardiomyocytes cultured on untreated PS serving as control. Viable cells (a) and fluorescent images of non-purified (b) and purified (c) neonatal rat cardiomyocytes cultured on the control PS for 3 days. Green: α-actinin, red: actin, blue: nuclei. Statistical analyses were realised using parametric t-test. ***p* < 0.01.

Quantification of live cells using the Muse® Count & Viability Kit showed that the number of viable cells was higher for N_2-treated surfaces but the difference did not reach statistically significant level with non-purified cardiomyocytes (Fig. 7a). Similarly, the control did not show statistical significance in the case of non-purified cardiomyocytes (Fig. 7a). This difference becomes more apparent in the case of the purified cardiomyocytes. As shown in Figure 7b, the number of viable cells was lower for O_2-treated samples, as well as the control, while the highest number of cells was calculated on the N_2-30 min treated surfaces. The number of viable cells remains similar even after 30 mins of treatment for N_2 samples, with a slight increase. Contrarily, the number of viable cells decrease for O_2 samples when 30 min plasma treatment samples are used in comparison to 20 min of treatment samples.

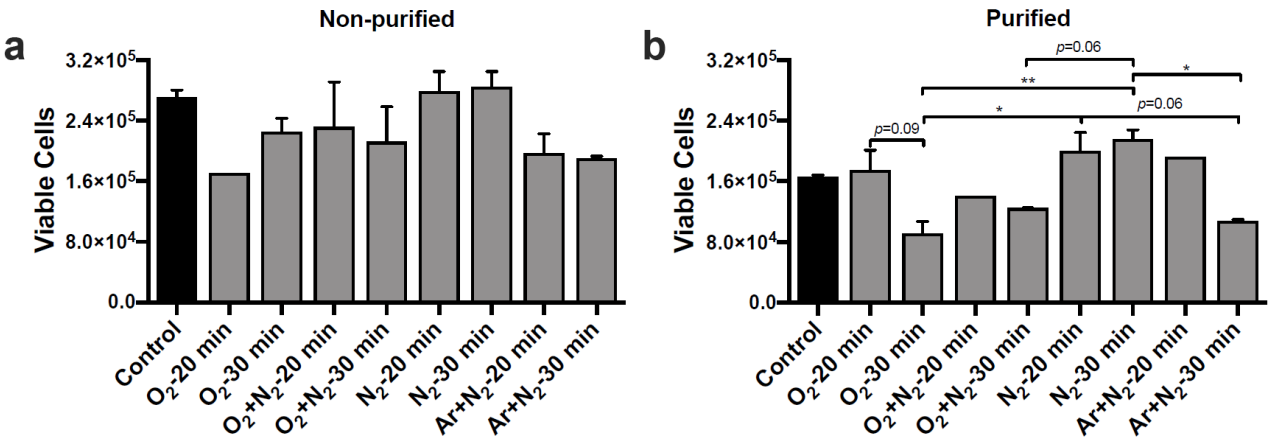

Fig. 7. Cell viability monitoring of primary cardiomyocytes cultured on different plasma treated PS. Non-purifed (A) and purified (B) neonatal rat cardiomyocytes cultured for 3 days on various plasma-treated PS, and live cells were quantified using the Muse® Count & Viability Kit. Statistical analyses were realised using one-way ANOVA. If a significant difference was found, Tukey's post hoc tests for multiple comparisons were used. *$p < 0.05$, **$p < 0.01$.

The shape of the cardiomyocytes that are growing on the plasma-treated PS samples was further analysed using confocal microscopy and SEM. The confocal microscopic images after immunostaining for α-actinin and nuclei of the purified cardiomyocytes, showed cells with normal shape, with well-organised sarcomeric structure, and well defined striations of their sarcomeres on the N_2-treated PS samples, which are much better than those cultured on the control (Fig. 8a,b). However, cells grown on the O_2-treated surfaces presented a round shape morphology without any sign of organisation of their α-actinin. It can also be observed that the higher O_2 plasma treatment time, further undermines the survival of the cardiomyocytes as it is shown in Figure 8c,d.

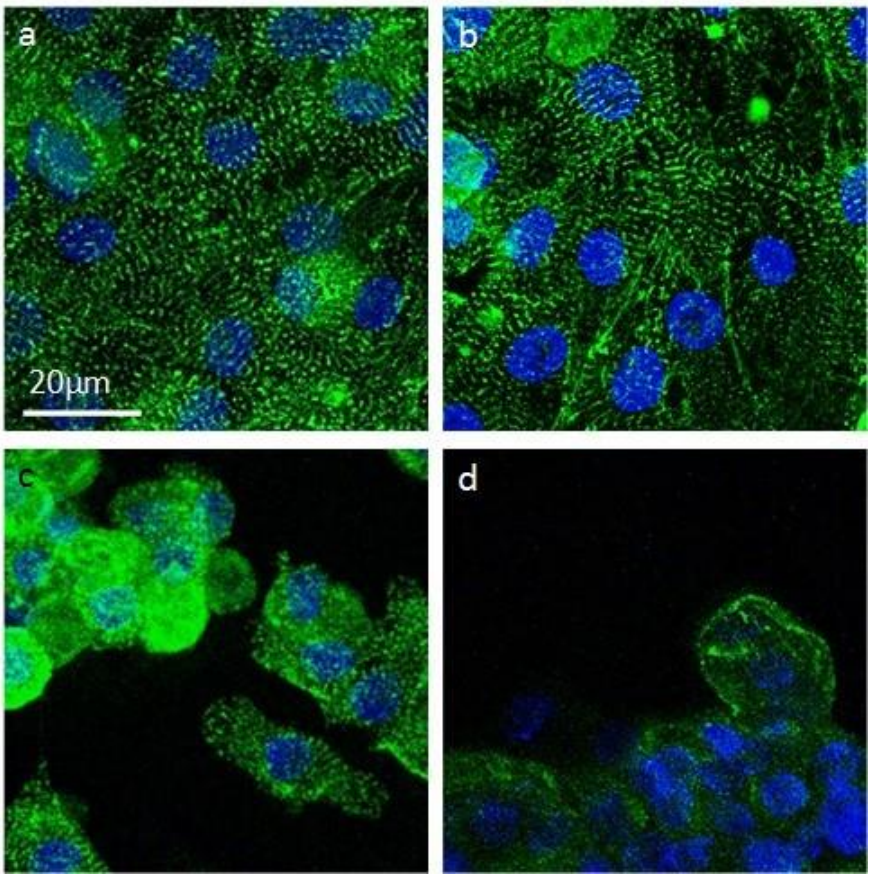

Fig. 8. Morphology of primary cardiomyocytes cultured on plasma-treated PS. Fluorescent images of purified neonatal rat cardiomyocytes cultured on plasma-treated PS for 3 days: (a)-(b) 20 and 30min of N_2 treatment, and (c)-(d) 20 and 30min of O_2 treatment, respectively. Green: α-actinin and blue: nuclei.

In line with the confocal microscopy results, cell morphology analysis by SEM indicated that cells grown on the N_2 surfaces had an elongated cylindrical shape (Fig. 9). However, cells grown on O_2 treated surfaces presented a round shape. The magnified images in the right column of Fig. 9 reveal in more detail the cell-substrate interaction. Details on how the pseudopodia of cardiomyocytes are attached to the PS surface can be clearly seen. It is evident in the images that the structured O_2-treated PS aided to the adhesion of cardiomyocytes as it allowed the pseudopodia to find increased surface to attach, but this fact was proven to be insufficient to allow them to spread and have their normal shape. Overall, these results clearly showcase the specificity of purified primary cardiomyocytes and their difficulty to adhere and expand in *in vitro* cultures. Indeed, the non-purified cardiomyocytes can adhere to all of the surfaces that were used in this study, even to the O_2-treated

ones (Fig. S9†). It appears that the N_2 plasma treatment favours cardiomyocytes' survival and spreading, via providing a combination of favourable nanotopography in the range of 50nm, as well as surface chemistry for the sample.

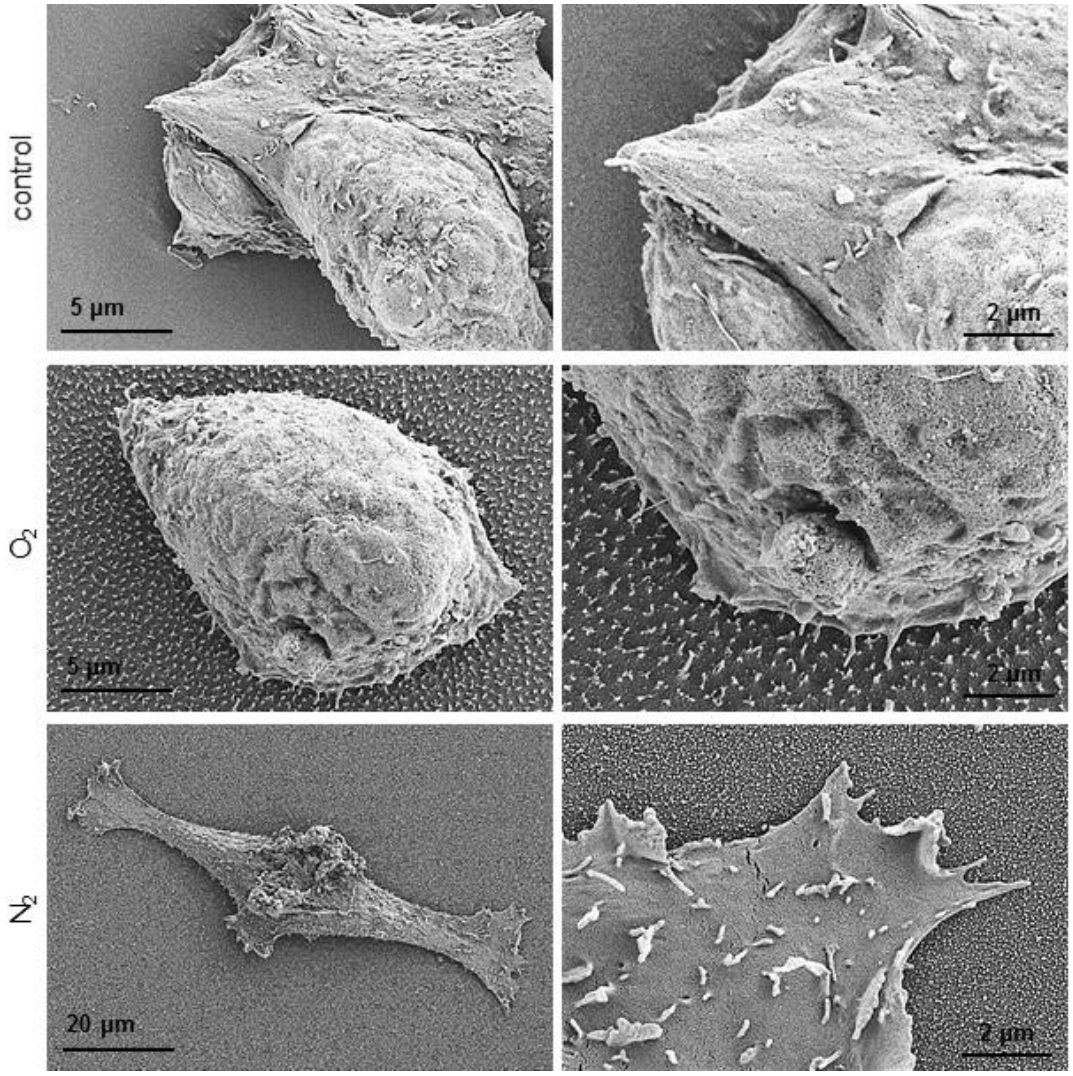

Fig. 9. SEM images of primary cardiomyocytes cultured on plasma-treated PS. Primary cardiomyocytes were cultured for three days on non-treated or on O_2 or N_2-treated PS.

4. Conclusion

In this work, a combined characterisation of both the morphology and surface chemistry is presented for numerous popular plasma treatments on PS. SEM results show that O_2 plasma creates dual scale roughness on the surface while N_2 plasma creates oval-shaped nanostructures. Mixtures of gasses showed that the resulting topography is mostly affected by the most chemical reactive ions, *i.e.* oxygen for oxygen mixtures and nitrogen for nitrogen mixtures. WCA measurements showed superhydrophilisation of all surfaces. The hydrophobic recovery though was much slower in the N_2 plasma treated samples. XPS shows interestingly oxygen peaks for both oxygen and N_2 treated samples, and as expected nitrogen peaks for N_2 treated samples. Increasing the plasma treatment time led to the increase of both oxygen and nitrogen species.

When H9c2 cells are cultured on the samples, analysis showed that the N_2 treated samples displayed a better behaviour than all the other plasma treatments both in terms of viability and morphology. Longer plasma treated samples promoted these findings even further. In the case of primary purified and non-purified cardiomyocytes, the viability of the cells is drastically improved in the case of the N_2 plasma treatment comparing to O_2 plasma treated surfaces. For the control the

purified cells indicated a worse viability comparing to the N_2 treated samples. The O_2 plasma treated samples provided a 'hostile' environment towards the cardiomyocytes, as both in the case of purified and not purified cardiomyocytes the number of cells dramatically decreased, especially in the case of the 30 minutes O_2 plasma treatment sample. Confocal microscopy showed the well-defined structure of striations of the sarcomeres of the cells only in the case of the N_2 treated sample, whereas in the case of O_2 treated sample as well as the control sample, the cell showed a circular morphology and loss of organisation of α-actinin. SEM images confirmed the same morphology of the cardiomyocytes with an elongated and spherical one for N_2 and O_2 plasma treated surfaces respectively.

Our results provide strong evidence on what is the desirable plasma treatment in the case of using PS for cardiac cells. Additionally, the outcome of our analysis overturns the common belief that O_2 plasma treatment provides an optimum tool to construct an appropriate microenvironment and conditions for cell culture in general. Although favourable towards surface hydrophilisation, here oxygen species are proven to not be able to provide the expected environment for cells, as viability, shape, and striations are not ideal for cardiac cell culture. Contrarily, N_2 plasma allows cardiac cells to perform their normal functions, leading to the conclusion that it produces a friendlier cellular environment. Moreover, the stability in hydrophilicity, thus in surface chemistry, of N_2 treated PS is an additional factor for concluding that this treatment is preferable in the case of culture studies. From all the above and from the SEM images that show pseudopodia and attachment of cells on all cases, one can clearly see that the cellular behaviour is mostly affected and led by the surface chemistry and that topography plays an ancillary role in the case of primary cardiomyocyte culture.

Our research can lead to the control of numerous cellular mechanisms by minimising effects of the culture surface and allowing the cardiac cells to develop in their natural shape, promoting their normal behaviour when cultured.

Declaration of Competing Interest

The authors declared that there is no conflict of interest.

Acknowledgements

This work was supported by the LabEx REVIVE (ANR-10-LABX-73), the Ile-de-France Region in the framework of the DIM Respore, the Île-de-France network of Excellence in Porous Solids and the AFM-Téléthon (contract number: 22142). MK acknowledges personal funding from the LabEx REVIVE and DIM Respore too. The authors also acknowledge IMPC from Sorbonne University (Institut des Matériaux de Paris Centre, FR CNRS 2482) and the C'Nano projects of the Region Ile-de-France, for Omicron XPS apparatus funding. The authors thank the personnel of the Photon Microscopy Facility of IBPS for helpful advice and technical assistance during microscopy image acquisition and analysis.

References

[1] J. Maul, B.G. Frushour, J.R. Kontoff, H. Eichenauer, K.-H. Ott, C. Schade, Polystyrene and Styrene Copolymers, in: Ullmann's Encycl. Ind. Chem., Wiley-VCH Verlag GmbH & Co. KGaA, Weinheim, Germany, 2007. https://doi.org/10.1002/14356007.a21_615.pub2.

[2] E. Imbert-laurenceau, M. Berger, G. Pavon-djavid, A. Jouan, Surface modification of polystyrene particles for specific antibody adsorption, 46 (2005) 1277–1285. https://doi.org/10.1016/j.polymer.2004.11.053.

[3] J.C. Capricho, K. Prasad, N. Hameed, M. Nikzad, N. Salim, Upcycling Polystyrene, Polymers (Basel). 14 (2022) 5010. https://doi.org/10.3390/polym14225010.

[4] L. Wang, L. Yan, P. Zhao, Y. Torimoto, M. Sadakata, Q. Li, Surface modification of polystyrene with atomic oxygen radical anions-dissolved solution, Appl. Surf. Sci. 254 (2008) 4191–4200. https://doi.org/10.1016/j.apsusc.2008.01.035.

[5] P. Rytlewski, M. Żenkiewicz, Laser-induced surface modification of polystyrene, Appl. Surf. Sci. 256 (2009) 857–861. https://doi.org/10.1016/j.apsusc.2009.08.075.

[6] D.S. Trentin, F. Bonatto, K.R. Zimmer, V.B. Ribeiro, A.L.S. Antunes, A.L. Barth, G. V. Soares, C. Krug, I.J.R. Baumvol, A.J. Macedo, N2/H2 plasma surface modifications of polystyrene inhibit the adhesion of multidrug resistant bacteria, Surf. Coatings Technol. 245 (2014) 84–91. https://doi.org/10.1016/j.surfcoat.2014.02.046.

[7] J. DENG, L. WANG, L. LIU, W. YANG, Developments and new applications of UV-induced surface graft polymerizations, Prog. Polym. Sci. 34 (2009) 156–193. https://doi.org/10.1016/j.progpolymsci.2008.06.002.

[8] D.F. Siqueira-Petri, G. Wenz, P. Schunk, T. Schimmel, M. Bruns, M.A. Dichtl, Surface modification of thin polystyrene films, Colloid Polym. Sci. 277 (1999) 673–679. https://doi.org/10.1007/s003960050439.

[9] P. Xue, Q. Li, L. Sun, L. Zhang, Z. Xu, C.M. Li, Y. Kang, A simple technique of constructing nano-roughened polydimethylsiloxane surface to enhance mesenchymal stem cell adhesion and proliferation, Microfluid. Nanofluidics. 22 (2018) 1. https://doi.org/10.1007/s10404-017-2014-4.

[10] D.H. Kim, D.W. Lee, J.Y. Oh, J. Won, D. Seo, Surface reformed anisotropic polystyrene-block -poly(ethylene- ran -butylene)- block -polystyrene- graft -maleic anhydride layer via ion-beam irradiation for liquid crystals, Polym. Adv. Technol. 33 (2022) 2581–2588. https://doi.org/10.1002/pat.5714.

[11] P. Slepička, N. Slepičková Kasálková, Z. Kolská, V. Švorčík, Surface Modification of Polymer Substrates for Biomedical Applications, in: Surf. Modif. Polym., Wiley-VCH Verlag GmbH & Co. KGaA, Weinheim, Germany, 2019: pp. 399–426. https://doi.org/10.1002/9783527819249.ch14.

[12] J. Wang, H. Ding, G. Duan, H. Zhou, C. Song, J. Pan, C. Li, Morphology-controllable gold hierarchically micro/nanostructured arrays prepared by electrodeposition on colloidal monolayer and their structurally related wettability, Chem. Phys. 523 (2019) 63–69. https://doi.org/10.1016/j.chemphys.2019.04.001.

[13] S. Park, H.Y. Cho, J.A. Yoon, Y. Kwak, A. Srinivasan, J.O. Hollinger, H. Paik, K. Matyjaszewski, Photo-Cross-Linkable Thermoresponsive Star Polymers Designed for Control of Cell-Surface Interactions, Biomacromolecules. 11 (2010) 2647–2652. https://doi.org/10.1021/bm100630f.

[14] R.A.N. Pertile, F.K. Andrade, C. Alves, M. Gama, Surface modification of bacterial cellulose by nitrogen-containing plasma for improved interaction with cells, Carbohydr. Polym. 82 (2010) 692–698. https://doi.org/10.1016/j.carbpol.2010.05.037.

[15] T. Desmet, R. Morent, N. De Geyter, C. Leys, E. Schacht, P. Dubruel, Nonthermal Plasma Technology as a Versatile Strategy for Polymeric Biomaterials Surface Modification: A Review, Biomacromolecules. 10 (2009) 2351–2378. https://doi.org/10.1021/bm900186s.

[16] W. Pfleging, M. Bruns, A. Welle, S. Wilson, Laser-assisted modification of polystyrene surfaces for cell culture applications, 253 (2007) 9177–9184. https://doi.org/10.1016/j.apsusc.2007.05.047.

[17] R. Günther, W. Caseri, C. Brändli, Copper Ions Absorbed on Acrylic-Acid-Grafted Polystyrene Enable Direct Bonding with Tunable Bonding Strength and Debonding on Demand, Polymers (Basel). 14 (2022) 5142. https://doi.org/10.3390/polym14235142.

[18] X. Zheng, L. Zhang, C. Jiang, J. Li, Y. Li, X. Liu, C. Li, Z. Wang, N. Zheng, Z. Fan, Acute effects of three surface-modified nanoplastics against Microcystis aeruginosa: Growth, microcystin production, and mechanisms, Sci. Total Environ. 855 (2023) 158906. https://doi.org/10.1016/j.scitotenv.2022.158906.

[19] D.V. Golubenko, A.B. Yaroslavtsev, Effect of current density, concentration of ternary electrolyte and type of cations on the monovalent ion selectivity of surface-sulfonated graft

anion-exchange membranes: modelling and experiment, J. Memb. Sci. 635 (2021) 119466. https://doi.org/10.1016/j.memsci.2021.119466.

[20] S.K. Schmitt, A.W. Xie, R.M. Ghassemi, D.J. Trebatoski, W.L. Murphy, P. Gopalan, Polyethylene Glycol Coatings on Plastic Substrates for Chemically Defined Stem Cell Culture, Adv. Healthc. Mater. 4 (2015) 1555–1564. https://doi.org/10.1002/adhm.201500191.

[21] E. Gogolides, V. Constantoudis, G. Kokkoris, D. Kontziampasis, K. Tsougeni, G. Boulousis, M. Vlachopoulou, A. Tserepi, Controlling roughness: from etching to nanotexturing and plasma-directed organization on organic and inorganic materials, J. Phys. D. Appl. Phys. 44 (2011) 174021. https://doi.org/10.1088/0022-3727/44/17/174021.

[22] D. Kontziampasis, G. Boulousis, A. Smyrnakis, K. Ellinas, A. Tserepi, E. Gogolides, Biomimetic, antireflective, superhydrophobic and oleophobic PMMA and PMMA-coated glass surfaces fabricated by plasma processing, Microelectron. Eng. 121 (2014) 33–38. https://doi.org/10.1016/j.mee.2014.02.027.

[23] A. Bourkoula, V. Constantoudis, D. Kontziampasis, P.S. Petrou, S.E. Kakabakos, A. Tserepi, E. Gogolides, Roughness threshold for cell attachment and proliferation on plasma micro-nanotextured polymeric surfaces: the case of primary human skin fibroblasts and mouse immortalized 3T3 fibroblasts, J. Phys. D. Appl. Phys. 49 (2016) 304002. https://doi.org/10.1088/0022-3727/49/30/304002.

[24] D. Kontziampasis, T. Trantidou, A. Regoutz, E.J. Humphrey, D. Carta, C.M. Terracciano, T. Prodromakis, Effects of Ar and O 2 Plasma Etching on Parylene C: Topography versus Surface Chemistry and the Impact on Cell Viability, Plasma Process. Polym. 13 (2016) 324–333. https://doi.org/10.1002/ppap.201500053.

[25] M. Kitsara, A. Blanquer, G. Murillo, V. Humblot, S. De Bragança Vieira, C. Nogués, E. Ibáñez, J. Esteve, L. Barrios, Permanently hydrophilic, piezoelectric PVDF nanofibrous scaffolds promoting unaided electromechanical stimulation on osteoblasts, Nanoscale. 11 (2019) 8906–8917. https://doi.org/10.1039/C8NR10384D.

[26] J. Oberländer, C. Champanhac, R. da Costa Marques, K. Landfester, V. Mailänder, Temperature, concentration, and surface modification influence the cellular uptake and the protein corona of polystyrene nanoparticles, Acta Biomater. 148 (2022) 271–278. https://doi.org/10.1016/j.actbio.2022.06.028.

[27] N. Singh, J. Chen, K.K. Koziol, K.R. Hallam, D. Janas, A.J. Patil, A. Strachan, J. G. Hanley, S.S. Rahatekar, Chitin and carbon nanotube composites as biocompatible scaffolds for neuron growth, Nanoscale. 8 (2016) 8288–8299. https://doi.org/10.1039/C5NR06595J.

[28] P.S. Arinda, D.J.D.H. Sandtjojo, D.D. Kamasi, S.P. Sakti, The characteristics of surface morphology on the polystyrene thin film using DC-bias oxygen plasma treatment, in: 2022: p. 070015. https://doi.org/10.1063/5.0072451.

[29] A. Vesel, R. Zaplotnik, M. Mozetič, G. Primc, Surface modification of PS polymer by oxygen-atom treatment from remote plasma: Initial kinetics of functional groups formation, Appl. Surf. Sci. 561 (2021) 150058. https://doi.org/10.1016/j.apsusc.2021.150058.

[30] M.-J. Wang, Y.-I. Chang, F. Poncin-Epaillard, Acid and basic functionalities of nitrogen and carbon dioxide plasma-treated polystyrene, Surf. Interface Anal. 37 (2005) 348–355. https://doi.org/10.1002/sia.2029.

[31] A.F. Novi, D.J.D.H. Santjojo, Masruroh, The Effect of Substrate Temperature on Surface Modification of Polystyrene by using Nitrogen Plasma, IOP Conf. Ser. Mater. Sci. Eng. 202 (2017) 012036. https://doi.org/10.1088/1757-899X/202/1/012036.

[32] Y. Chen, Q. Gao, H. Wan, J. Yi, Y. Wei, P. Liu, Applied Surface Science Surface modification and biocompatible improvement of polystyrene film by Ar , O 2 and Ar + O 2 plasma, Appl. Surf. Sci. 265 (2013) 452–457. https://doi.org/10.1016/j.apsusc.2012.11.027.

[33] X. Li, F. Lu, M. Cocca, K. Vega, A. Fleischer, A. Bailey, M. Toro, S. Sachdev, T. Debies, M.

Mehan, S. Gupta, G. Takacs, Surface Modification of Polystyrene with O Atoms Produced Downstream from an Ar/O2 Microwave Plasma, Technologies. 6 (2018) 21. https://doi.org/10.3390/technologies6010021.

[34] A.W.S. Ramsey, W. Hertl, E.D. Nowlan, N.J. Binkowski, Surface Treatments and cell attachment, In Vitro. 20 (1984) 802–808.

[35] P. Luan, V.S.S.K. Kondeti, A.J. Knoll, P.J. Bruggeman, G.S. Oehrlein, Effect of water vapor on plasma processing at atmospheric pressure: Polymer etching and surface modification by an Ar/H 2 O plasma jet, J. Vac. Sci. Technol. A. 37 (2019) 031305. https://doi.org/10.1116/1.5092272.

[36] F. Kong, C. Chang, Y. Ma, C. Zhang, C. Ren, T. Shao, Surface modifications of polystyrene and their stability: A comparison of DBD plasma deposition and direct fluorination, Appl. Surf. Sci. 459 (2018) 300–308. https://doi.org/10.1016/j.apsusc.2018.07.211.

[37] A.S. Chiper, Tailoring the working gas flow to improve the surface modification of plasma-treated polymers, Mater. Lett. 305 (2021) 130832. https://doi.org/10.1016/j.matlet.2021.130832.

[38] T.-H. Chen, F.-Y. Chung, W.-F. Jiang, C. Huang, A study of plasma power effects on surface activation of polystyrene, Vacuum. 186 (2021) 110069. https://doi.org/10.1016/j.vacuum.2021.110069.

[39] M.K.M. Amorim, E.C. Rangel, R. Landers, S.F. Durrant, Effects of cold SF6 plasma treatment on a-C:H, polypropylene and polystyrene, Surf. Coatings Technol. 385 (2020) 125398. https://doi.org/10.1016/j.surfcoat.2020.125398.

[40] P. Surya Arinda, D. Joseph Djoko Herry Santjojo, M. Masruroh, S. Purnomo Sakti, Stability of Polystyrene Film Surface Wettability Modified Using Oxygen Plasma, Mater. Today Proc. 13 (2019) 24–29. https://doi.org/10.1016/j.matpr.2019.03.181.

[41] H. Suzuki, K. Kasai, Y. Kimura, S. Miyata, UV/ozone surface modification combined with atmospheric pressure plasma irradiation for cell culture plastics to improve pluripotent stem cell culture, Mater. Sci. Eng. C. 123 (2021) 112012. https://doi.org/10.1016/j.msec.2021.112012.

[42] S. Haubenwallner, M. Katschnig, U. Fasching, S. Patz, C. Trattnig, N. Andraschek, G. Grünbacher, M. Absenger, S. Laske, C. Holzer, W. Balika, M. Wagner, U. Schäfer, Effects of the polymeric niche on neural stem cell characteristics during primary culturing, J. Mater. Sci. Mater. Med. 25 (2014) 1339–1355. https://doi.org/10.1007/s10856-014-5155-y.

[43] M. Kitsara, O. Agbulut, D. Kontziampasis, Y. Chen, P. Menasché, Fibers for hearts: A critical review on electrospinning for cardiac tissue engineering, Acta Biomater. 48 (2017) 20–40. https://doi.org/10.1016/j.actbio.2016.11.014.

[44] M. Kitsara, D. Kontziampasis, O. Agbulut, Y. Chen, Heart on a chip: Micro-nanofabrication and microfluidics steering the future of cardiac tissue engineering, Microelectron. Eng. 203–204 (2019) 44–62. https://doi.org/10.1016/j.mee.2018.11.001.

[45] K. Ellinas, A. Tserepi, E. Gogolides, Superhydrophobic Fabrics with Mechanical Durability Prepared by a Two-Step Plasma Processing Method, Coatings. 8 (2018) 351. https://doi.org/10.3390/coatings8100351.

[46] K. Ellinas, E. Gogolides, Ultra-low friction, superhydrophobic, plasma micro-nanotextured fluorinated ethylene propylene (FEP) surfaces, Micro Nano Eng. 14 (2022) 100104. https://doi.org/10.1016/j.mne.2022.100104.

[47] K. Tsougeni, A. Tserepi, V. Constantoudis, E. Gogolides, Plasma Nanotextured PMMA Surfaces for Protein Arrays : Increased Protein Binding and Enhanced Detection Sensitivity, 26 (2010) 13883–13891. https://doi.org/10.1021/la101957w.

[48] D.B. Graves, D. Humbird, Surface chemistry associated with plasma etching processes, Appl. Surf. Sci. 192 (2002) 72–87. https://doi.org/10.1016/S0169-4332(02)00021-1.

[49] A.-L. Thomann, N. Semmar, R. Dussart, J. Mathias, V. Lang, Diagnostic system for

plasma/surface energy transfer characterization, Rev. Sci. Instrum. 77 (2006) 033501. https://doi.org/10.1063/1.2166467.

[50] K. Ostrikov, E.C. Neyts, M. Meyyappan, Plasma nanoscience: from nano-solids in plasmas to nano-plasmas in solids, Adv. Phys. 62 (2013) 113–224. https://doi.org/10.1080/00018732.2013.808047.

[51] G. Memos, E. Lidorikis, G. Kokkoris, Roughness Evolution and Charging in Plasma-Based Surface Engineering of Polymeric Substrates: The Effects of Ion Reflection and Secondary Electron Emission, Micromachines. 9 (2018) 415. https://doi.org/10.3390/mi9080415.

[52] G. Memos, E. Lidorikis, G. Kokkoris, The interplay between surface charging and microscale roughness during plasma etching of polymeric substrates, J. Appl. Phys. 123 (2018) 073303. https://doi.org/10.1063/1.5018313.

[53] S. Mouchtouris, G. Kokkoris, Multiscale Modeling of Low Pressure Plasma Etching Processes: Linking the Operating Parameters of the Plasma Reactor with Surface Roughness Evolution, Plasma Process. Polym. 14 (2017) 1600147. https://doi.org/10.1002/ppap.201600147.

[54] G. Kokkoris, E. Gogolides, The potential of ion-driven etching with simultaneous deposition of impurities for inducing periodic dots on surfaces, J. Phys. D. Appl. Phys. 45 (2012) 165204. https://doi.org/10.1088/0022-3727/45/16/165204.

[55] Y. Li, J.Q. Pham, K.P. Johnston, P.F. Green, Contact Angle of Water on Polystyrene Thin Films: Effects of CO 2 Environment and Film Thickness, Langmuir. 23 (2007) 9785–9793. https://doi.org/10.1021/la0636311.

[56] N. Recek, M. Mozetic, M. Jaganjac, L. Milkovic, N. Zarkovic, A. Vesel, Adsorption of Proteins and Cell Adhesion to Plasma Treated Polymer Substrates, Int. J. Polym. Mater. Polym. Biomater. 63 (2014) 685–691. https://doi.org/10.1080/00914037.2013.854243.

[57] O.M. Ba, P. Marmey, K. Anselme, A.C. Duncan, A. Ponche, Colloids and Surfaces B : Biointerfaces Surface composition XPS analysis of a plasma treated polystyrene : Evolution over long storage periods, Colloids Surfaces B Biointerfaces. 145 (2016) 1–7. https://doi.org/10.1016/j.colsurfb.2016.04.026.

[58] E.H. Lock, D.Y. Petrovykh, P. Mack, T. Carney, R.G. White, S.G. Walton, R.F. Fernsler, Surface Composition, Chemistry, and Structure of Polystyrene Modified by Electron-Beam-Generated Plasma, Langmuir. 26 (2010) 8857–8868. https://doi.org/10.1021/la9046337.

[59] O. Rosseler, M. Sleiman, V.N. Montesinos, A. Shavorskiy, V. Keller, N. Keller, M.I. Litter, H. Bluhm, M. Salmeron, H. Destaillats, Chemistry of NO x on TiO 2 Surfaces Studied by Ambient Pressure XPS: Products, Effect of UV Irradiation, Water, and Coadsorbed K +, J. Phys. Chem. Lett. 4 (2013) 536–541. https://doi.org/10.1021/jz302119g.

[60] J. Hescheler, R. Meyer, S. Plant, D. Krautwurst, W. Rosenthal, G. Schultz, Morphological, biochemical, and electrophysiological characterization of a clonal cell (H9c2) line from rat heart., Circ. Res. 69 (1991) 1476–1486. https://doi.org/10.1161/01.RES.69.6.1476.

[61] J.L. Bays, K.A. DeMali, Vinculin in cell–cell and cell–matrix adhesions, Cell. Mol. Life Sci. 74 (2017) 2999–3009. https://doi.org/10.1007/s00018-017-2511-3.

[62] W.H. Ziegler, R.C. Liddington, D.R. Critchley, The structure and regulation of vinculin, Trends Cell Biol. 16 (2006) 453–460. https://doi.org/10.1016/j.tcb.2006.07.004.

[63] H.-A. Pan, Y.-C. Hung, Y.-P. Sui, G.S. Huang, Topographic control of the growth and function of cardiomyoblast H9c2 cells using nanodot arrays, Biomaterials. 33 (2012) 20–28. https://doi.org/10.1016/j.biomaterials.2011.09.054.

26 (2010) 13883–13891. https://doi.org/10.1021/la101957w.

[48] D.B. Graves, D. Humbird, Surface chemistry associated with plasma etching processes, Appl. Surf. Sci. 192 (2002) 72–87. https://doi.org/10.1016/S0169-4332(02)00021-1.

[49] A.-L. Thomann, N. Semmar, R. Dussart, J. Mathias, V. Lang, Diagnostic system for plasma/surface energy transfer characterization, Rev. Sci. Instrum. 77 (2006) 033501. https://doi.org/10.1063/1.2166467.

[50] K. Ostrikov, E.C. Neyts, M. Meyyappan, Plasma nanoscience: from nano-solids in plasmas to nano-plasmas in solids, Adv. Phys. 62 (2013) 113–224. https://doi.org/10.1080/00018732.2013.808047.

[51] G. Memos, E. Lidorikis, G. Kokkoris, Roughness Evolution and Charging in Plasma-Based Surface Engineering of Polymeric Substrates: The Effects of Ion Reflection and Secondary Electron Emission, Micromachines. 9 (2018) 415. https://doi.org/10.3390/mi9080415.

[52] G. Memos, E. Lidorikis, G. Kokkoris, The interplay between surface charging and microscale roughness during plasma etching of polymeric substrates, J. Appl. Phys. 123 (2018) 073303. https://doi.org/10.1063/1.5018313.

[53] S. Mouchtouris, G. Kokkoris, Multiscale Modeling of Low Pressure Plasma Etching Processes: Linking the Operating Parameters of the Plasma Reactor with Surface Roughness Evolution, Plasma Process. Polym. 14 (2017) 1600147. https://doi.org/10.1002/ppap.201600147.

[54] G. Kokkoris, E. Gogolides, The potential of ion-driven etching with simultaneous deposition of impurities for inducing periodic dots on surfaces, J. Phys. D. Appl. Phys. 45 (2012) 165204. https://doi.org/10.1088/0022-3727/45/16/165204.

[55] Y. Li, J.Q. Pham, K.P. Johnston, P.F. Green, Contact Angle of Water on Polystyrene Thin Films: Effects of CO 2 Environment and Film Thickness, Langmuir. 23 (2007) 9785–9793. https://doi.org/10.1021/la0636311.

[56] N. Recek, M. Mozetic, M. Jaganjac, L. Milkovic, N. Zarkovic, A. Vesel, Adsorption of Proteins and Cell Adhesion to Plasma Treated Polymer Substrates, Int. J. Polym. Mater. Polym. Biomater. 63 (2014) 685–691. https://doi.org/10.1080/00914037.2013.854243.

[57] O.M. Ba, P. Marmey, K. Anselme, A.C. Duncan, A. Ponche, Colloids and Surfaces B : Biointerfaces Surface composition XPS analysis of a plasma treated polystyrene : Evolution over long storage periods, Colloids Surfaces B Biointerfaces. 145 (2016) 1–7. https://doi.org/10.1016/j.colsurfb.2016.04.026.

[58] E.H. Lock, D.Y. Petrovykh, P. Mack, T. Carney, R.G. White, S.G. Walton, R.F. Fernsler, Surface Composition, Chemistry, and Structure of Polystyrene Modified by Electron-Beam-Generated Plasma, Langmuir. 26 (2010) 8857–8868. https://doi.org/10.1021/la9046337.

[59] O. Rosseler, M. Sleiman, V.N. Montesinos, A. Shavorskiy, V. Keller, N. Keller, M.I. Litter, H. Bluhm, M. Salmeron, H. Destaillats, Chemistry of NO x on TiO 2 Surfaces Studied by Ambient Pressure XPS: Products, Effect of UV Irradiation, Water, and Coadsorbed K +, J. Phys. Chem. Lett. 4 (2013) 536–541. https://doi.org/10.1021/jz302119g.

[60] J. Hescheler, R. Meyer, S. Plant, D. Krautwurst, W. Rosenthal, G. Schultz, Morphological, biochemical, and electrophysiological characterization of a clonal cell (H9c2) line from rat heart., Circ. Res. 69 (1991) 1476–1486. https://doi.org/10.1161/01.RES.69.6.1476.

[61] J.L. Bays, K.A. DeMali, Vinculin in cell–cell and cell–matrix adhesions, Cell. Mol. Life Sci. 74 (2017) 2999–3009. https://doi.org/10.1007/s00018-017-2511-3.

[62] W.H. Ziegler, R.C. Liddington, D.R. Critchley, The structure and regulation of vinculin, Trends Cell Biol. 16 (2006) 453–460. https://doi.org/10.1016/j.tcb.2006.07.004.

[63] H.-A. Pan, Y.-C. Hung, Y.-P. Sui, G.S. Huang, Topographic control of the growth and function of cardiomyoblast H9c2 cells using nanodot arrays, Biomaterials. 33 (2012) 20–28. https://doi.org/10.1016/j.biomaterials.2011.09.054.